

Magnetic field induced anisotropy of ^{139}La spin-lattice relaxation rates in stripe ordered $\text{La}_{1.875}\text{Ba}_{0.125}\text{CuO}_4$

S.-H. Baek,^{1,*} Y. Utz,^{1,2} M. Hückner,³ G. D. Gu,³ B. Büchner,^{1,2} and H.-J. Grafe¹

¹*IFW-Dresden, Institute for Solid State Research, PF 270116, 01171 Dresden, Germany*

²*Institut für Festkörperphysik, Technische Universität Dresden, 01062 Dresden, Germany*

³*Condensed Matter Physics and Materials Science Department,
Brookhaven National Laboratory, Upton, New York 11973, USA*

(Dated: October 27, 2015)

We report ^{139}La nuclear magnetic resonance studies performed on a $\text{La}_{1.875}\text{Ba}_{0.125}\text{CuO}_4$ single crystal. The data show that the structural phase transitions (high-temperature tetragonal \rightarrow low-temperature orthorhombic \rightarrow low-temperature tetragonal phase) are of the displacive type in this material. The ^{139}La spin-lattice relaxation rate T_1^{-1} sharply upturns at the charge-ordering temperature $T_{\text{CO}} = 54$ K, indicating that charge order triggers the slowing down of spin fluctuations. Detailed temperature and field dependencies of the T_1^{-1} below the spin-ordering temperature $T_{\text{SO}} = 40$ K reveal the development of enhanced spin fluctuations in the spin-ordered state for $H \parallel [001]$, which are completely suppressed for large fields along the CuO_2 planes. Our results shed light on the unusual spin fluctuations in the charge and spin stripe ordered lanthanum cuprates.

Numerous diffraction experiments have established the unidirectional spin/charge stripe model^{1–7} in the single-layer lanthanum-based cuprates, $\text{La}_{2-x}(\text{Ba},\text{Sr})_x\text{CuO}_4$ and $\text{La}_{2-x-y}\text{M}_y\text{Sr}_x\text{CuO}_4$ ($\text{M} = \text{Nd}, \text{Eu}$). The simple stripe picture, however, misses the leading electronic instability of stripe order and its relation to superconductivity. For example, it is largely unclear how charge order preceding spin order evolves to uniaxially modulated charge/spin stripe order.

X-ray diffraction experiments in high magnetic fields have shown that charge order is enhanced when superconductivity is suppressed by the magnetic field. However, in 1/8 doped $\text{La}_{1.875}\text{Ba}_{0.125}\text{CuO}_4$ where the stripe order is most stable and bulk superconductivity is absent already in the zero field, high magnetic fields have little effect on the charge order.⁸ Not much is known about anisotropic effects of magnetic fields applied along $[001]$ and $[100]$. Measurements of the static susceptibility indicate that the spin order is stabilized for high magnetic fields $H \parallel [100]$. Furthermore, a spin flop occurs at a magnetic field $H \geq 6$ T along this direction.⁹ Nuclear magnetic resonance (NMR) evidences unusual glassy spin fluctuations (SFs) below the spin-ordering temperature,^{10–15} but whether these spin fluctuations are related to charge order and whether there are anisotropy effects are not known.

Another issue of current research is the coupling of the charge order to the lattice. It is widely believed that the low-temperature orthorhombic (LTO) \rightarrow low-temperature tetragonal (LTT) structural phase transition has a profound effect on the stabilization of static charge/spin order which then suppresses superconductivity.^{16,17} Recent studies show that long range LTT ordering may not be essential for stripe order, but that local distortions may be enough to pin charge order.^{5,6,18–21} This indicates that the coupling mechanism among the lattice, spin/charge stripes, and superconductivity is far more complex and remains to be fully understood.

NMR is an ideal technique to investigate such a complex coupling mechanism, because it probes the local spin/charge environment surrounding a nucleus, in particular, low-frequency spin fluctuations associated with various phase transitions. Since the ^{63}Cu is too strongly influenced by the Cu moments leading to the wipeout of the NMR signal,^{10,12,22} the ^{139}La nucleus is better suited to investigate the stripe phase and the structural phase transitions (SPTs).^{11,14,23–25}

Here, we show by means of ^{139}La NMR that additional spin fluctuations develop in the spin-ordered state. These SFs are strongly anisotropic in large magnetic fields: applied along the CuO_2 planes, the large magnetic fields lead to a suppression of these additional SFs, and static hyperfine fields lead to a broadening and loss of the ^{139}La signal intensity. In contrast, magnetic fields perpendicular to the CuO_2 planes have a weak effect on the spin fluctuations, and an additional relaxation mechanism enhances the ^{139}La nuclear spin-lattice relaxation. The observed anisotropy goes along with the enhanced spin order for a magnetic field parallel to the CuO_2 planes.⁹ Our experiments also allowed for a detailed look at the local crystal structure, which has been the subject of a long debate. We find that structural phase transitions in $\text{La}_{1.875}\text{Ba}_{0.125}\text{CuO}_4$ are of the displacive type, locally probing the average structure given by diffraction studies.

The $\text{La}_{1.875}\text{Ba}_{0.125}\text{CuO}_4$ (LBCO:1/8) single crystal was grown with the traveling solvent floating zone method described in Ref. 26. The sample was accurately aligned along the magnetic field using a goniometer. ^{139}La (nuclear spin $I = 7/2$) NMR spectra were obtained by sweeping frequency at a fixed external field (H) in the temperature (T) range 10 — 300 K.²⁷ Spin-echo signals each were taken by shifting 50 kHz and their Fourier-transformed spectra were summed up to give rise to the full spectrum. Since the range of the sweeping frequency is quite narrow, i.e., much less than 2% of the Larmor frequency, the frequency correction was not made.

The spin-lattice relaxation rates T_1^{-1} were measured at the central transition ($+1/2 \leftrightarrow -1/2$) of ^{139}La by monitoring the recovery of the echo signal after a saturating single $\pi/2$ pulse which, depending on the experimental conditions, ranges from 2 to 4 μs . When the ^{139}La spectral width becomes broader at low temperatures, we carefully carried out the T_1 measurements to avoid any spectral diffusion. Then the following formula was used to fit the relaxation data to obtain T_1^{-1} :

$$1 - \frac{M(t)}{M(\infty)} = a \left(\frac{1}{84} e^{-(t/T_1)^\beta} + \frac{3}{44} e^{-(6t/T_1)^\beta} + \frac{75}{364} e^{-(15t/T_1)^\beta} + \frac{1225}{1716} e^{-(28t/T_1)^\beta} \right), \quad (1)$$

where M is the nuclear magnetization and a is a fitting parameter that is ideally one. β is the stretching exponent, which becomes less than unity when T_1^{-1} is spatially distributed, for example, in a spin glass.^{15,28}

Figure 1 shows the ^{139}La NMR central transition ($1/2 \leftrightarrow -1/2$) as a function of T obtained at $H = 10.7$ T applied along the crystallographic directions $[001]$ and $[100]$ of the high-temperature tetragonal (HTT) unit cell. Different colors of spectra denote different structural phases. For $H \parallel [001]$, the ^{139}La NMR line is quite narrow (full width at half maximum ~ 30 kHz) and almost independent of T in the HTT phase. Just below the $\text{HTT} \rightarrow \text{LTO}$ transition temperature T_{HT} , the ^{139}La line undergoes an anomalous change and, upon further cooling, continues to broaden and shift to lower frequency. The T evolution of the ^{139}La resonance frequency ν_0 through T_{HT} can be explained in terms of a second-order quadrupole shift which depends on the angle between the principal axis of the electric field gradient (i.e., the axis of V_{zz}) and H :

$$\nu_0 = \gamma_n(1 + \mathcal{K})H + \frac{15\nu_Q^2}{16\nu_0} [1 - \cos^2(\theta \pm \alpha)] [1 - 9\cos^2(\theta \pm \alpha)], \quad (2)$$

where γ_n is the nuclear gyromagnetic ratio, \mathcal{K} is the Knight shift, ν_Q is the quadrupole frequency, θ is the angle between $[001]$ and H , and α is the tilt angle of the CuO_6 octahedra with respect to $[001]$. Since $\theta = 0$ for $H \parallel [001]$ and \mathcal{K} for ^{139}La is very small in La-based cuprates,²⁴ the abrupt decrease of ν_0 below T_{HT} indicates that α of the second term in Eq. (2) becomes non-zero and gradually increases with decreasing T in the LTO phase. The much larger linewidth in the LTT phase is then ascribed to local tilt disorder, i.e., a spatial distribution of α .

This is strong evidence that the $\text{HTT} \rightarrow \text{LTO}$ transition can be described as a transition from flat CuO_2 planes in the HTT phase to a phase with tilted CuO_6 octahedra.²⁴ Note that we do not observe LTT-type tilt fluctuations persisting through the transitions, as has been found recently by a combination of neutron powder diffraction and inelastic neutron scattering,²⁹ most likely

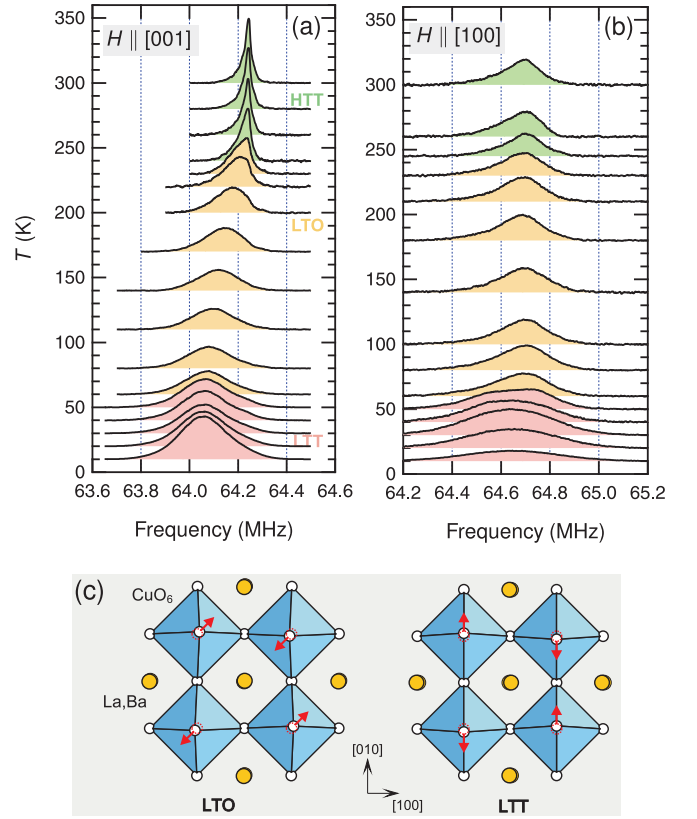


FIG. 1. ^{139}La NMR central transition spectrum as a function of T at 10.7 T applied along (a) $[001]$ and (b) $[100]$ in the HTT setting. The anomalous changes of the ^{139}La spectrum were observed at T_{HT} for $H \parallel [001]$ and at T_{LT} for $H \parallel [100]$, respectively. Below T_{SO} , the signal intensity becomes strongly anisotropic at low T . Both Boltzmann- and T_2 -corrections were made for the signal intensities. (c) Top view of LTO and LTT phases with one CuO_2 plane in the average structure of doped La_2CuO_4 . The arrows denote the tilt direction of the CuO_6 octahedra.

due to the different time scales of neutron-scattering and NMR experiments. For NMR linewidth measurements, fluctuations on a 10^{-2} ms timescale are already enough to average out the effects on the resonance lines.

However, our results are in agreement with the average structure from conventional diffraction studies,^{30–33} rather than the *local structure* model which proposes an order-disorder type transition.^{34–38} In the average structure model there is no tilt of the CuO_6 octahedra in the HTT phase, and the $\text{HTT} \rightarrow \text{LTO}$ transition is determined basically by the tilt angle of the octahedra. At the $\text{LTO} \rightarrow \text{LTT}$ transition, the tilt axis rotates by 45° in this model. On the other hand, in the local structure model the LTO structure is built up from the coherent spatial superposition of local LTT structures. Here, the tilt axis does not rotate at the $\text{LTO} \rightarrow \text{LTT}$ transition, and does not vanish at the $\text{HTT} \rightarrow \text{LTO}$ transition, which is not consistent with our data. Note, however, that for $H \parallel [100]$ ($\theta = 90^\circ$), the quadrupole broadening is very

large and obscures the tilting effect at T_{HT} . On the other hand, through the LTO \rightarrow LTT transition at T_{LT} , only for $H \parallel [100]$ is a clear anomaly observed. This observation as well is consistent with the average structure model. As illustrated in Fig. 1(c), when $H \parallel [100]$, the rotation of the octahedral tilt direction below T_{LT} should lead to a change of the direction of V_{zz} with respect to H . This is different from the case of $H \parallel [001]$ where α remains the same. We conclude that all structural phase transitions in Ba-doped La_2CuO_4 are in agreement with the average structure model.

The dynamic properties of the structural phase transitions and, in particular, of the spin fluctuations in the stripe ordered phase can be probed by the ^{139}La spin lattice relaxation rate T_1^{-1} . Figure 2(a) shows T_1^{-1} as a function of T at $H = 10.7$ T applied along $[001]$ and $[100]$, revealing sharp anomalies at T_{HT} and T_{LT} regardless of the field orientation. While the sharp peak at T_{HT} represents the thermodynamic critical mode associated with the HTT \rightarrow LTO transition, the rapid upturn at T_{LT} is most likely not caused by the LTO \rightarrow LTT transition itself, because T_1^{-1} is expected to *drop* sharply below T_{LT} , as was detected in $\text{La}_{1.8-x}\text{Eu}_{0.2}\text{Sr}_x\text{CuO}_4$ (LESCO).^{12,25} Indeed, a close look at Fig. 2(b) implies that the rapid upturn of T_1^{-1} by up to three orders of magnitude is most likely due to the spin ordering at 40 K. The T_1^{-1} upturn starts at the charge ordering temperature³⁹ $T_{CO} \sim T_{LT} \sim 54$ K suggesting that the charge ordering triggers the critical slowing down of SFs toward spin ordering.^{13,40}

Further, in Fig. 2(b) the field dependence of T_1^{-1} reveals interesting features in the stripe phase. In the temperature range $T_{SO} < T \leq T_{CO}$, despite the huge enhancement of T_1^{-1} by more than three orders of magnitude, $T_1^{-1}(T)$ is independent of orientation and strength of H . This suggests that the spin fluctuations are still isotropic and independent of H above T_{SO} , consistent with spin fluctuations of a two-dimensional (2D) quantum Heisenberg antiferromagnet or an effective spin-liquid state.⁴¹ On the other hand, the static susceptibility indicates that the spin dimensionality is already effectively reduced from 2D Heisenberg to 2D XY below T_{CO} .⁹ However, once the spins are ordered below $T_{SO} = 40$ K, $T_1^{-1}(T)$ also reveals a strongly anisotropic field dependence.

At 10.7 T $\parallel [100]$, $T_1^{-1}(T)$ displays the expected behavior for slow spin dynamics driven by conventional antiferromagnetic (AFM) correlations with a glassy nature: on the low temperature side, T_1^{-1} decreases steeply consistent with a conventional Bloembergen, Purcell, and Pound (BPP) mechanism.^{11,12} In contrast, for small fields parallel to $[100]$ as well as for all studied fields $H \parallel [001]$, the relaxation rate remains significantly enhanced below T_{SO} . This enhanced relaxation has already been observed in the stripe ordered phase of L(E)SCO, and led the authors to modify or even abandon the simple BPP model.^{11,12,14,15} Our results show that the spin-lattice relaxation deviates from the simple BPP model

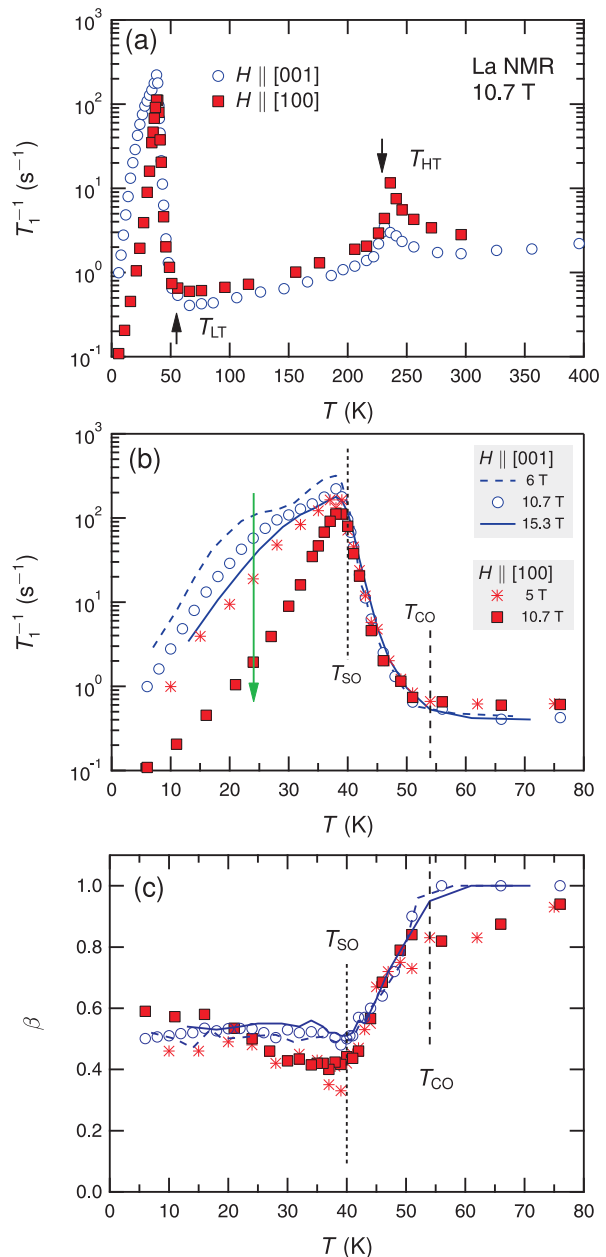


FIG. 2. (a) T dependence of ^{139}La T_1^{-1} at 10.7 T applied along $[001]$ and $[100]$. (b) T_1^{-1} vs T at various magnetic fields H . The onset of the T_1^{-1} upturn coincides with T_{CO} independent of H . Only below T_{SO} is the strong dependence of T_1^{-1} on the strength and orientation of H observed. The green arrow indicates the temperature where a detailed field dependence has been measured. (c) Stretching exponent β as a function of T and H , which correlated with T_1^{-1} .

for low fields and for $H \parallel [001]$. A possible reason for this deviation is that the field along the planes stabilizes the spin order.⁹ Small fields or a field perpendicular to the planes allow for the peculiar spin fluctuations that lead to the enhanced spin lattice relaxation and deviation from the simple BPP model below T_{SO} , as will be discussed in detail below.

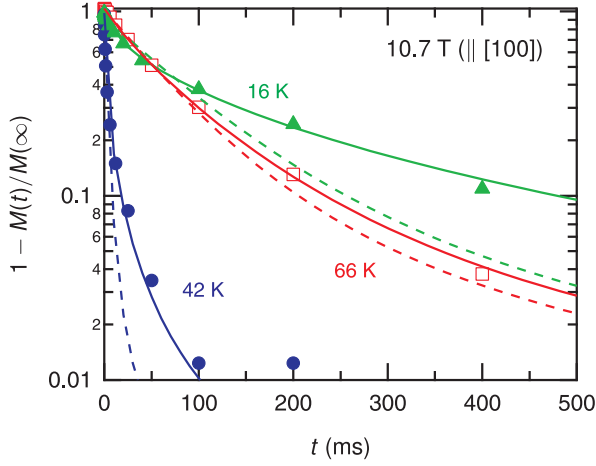


FIG. 3. Relaxation curves of nuclear magnetization M for $T = 16, 42$, and 66 K at 10.7 T parallel to $[100]$. The solid and dashed lines are fits by Eq. (1) with β as a free parameter and with $\beta = 1$, respectively. See text for details.

Another fingerprint of glassy spin dynamics besides the (modified) BPP behavior, and a measure of a distribution of spin-lattice relaxation rates, is a stretching exponent β that deviates from one [see Eq. (1)]. β is presented in Fig. 2(c) as a function of H and T , and exhibits distinct changes at T_{CO} and T_{SO} , which correlate with $T_1^{-1}(T)$. The decrease of β below T_{CO} indicates that the charge ordering initiates the distribution of T_1^{-1} , and therefore of the inhomogeneous spin fluctuations. Below T_{SO} , $\beta(T)$ is weakly T and H dependent, i.e. a large, but T -independent distribution of spin fluctuations is still present.¹⁵ The anisotropic behavior of T_1^{-1} below T_{SO} is, however, not reflected in the distribution of spin lattice relaxation rates.

Since the multi-exponential relaxation function [Eq. (1)] is complicated and the values of T_1^{-1} obtained from a stretched fit are not the average T_1^{-1} ,¹⁵ we show in Fig. 3 typical recovery curves and fits for $T = 16, 42$, and 66 K. Clearly, a stretching exponent β is needed to account for the distribution of spin-lattice relaxation rates. On the other hand, the values of T_1^{-1} fitted with or without the stretching exponent do not deviate substantially: At 66 K, $T_1 = 1677$ ms with $\beta = 0.87$, and $T_1 = 1660$ ms ($\beta = 1$). At 16 K $T_1 = 2208$ ms with $\beta = 0.58$, and $T_1 = 2194$ ms ($\beta = 1$). For fast relaxation at 42 K, the deviations of T_1^{-1} depending on the stretching exponent are larger: $T_1 = 49$ ms ($\beta = 0.46$) and $T_1 = 72$ ms ($\beta = 1$). However, when plotting T_1^{-1} on a log scale as in Fig. 2(b), the deviation is hardly larger than the point size for 42 K. Therefore, the stretched relaxation has no impact on the main findings of our work.

In order to gain a better understanding of the anisotropic SFs, we examined in detail the field dependence of T_1^{-1} at a fixed temperature of 24 K, which is shown in Fig. 4. Figure 2(b) already revealed that $T_1^{-1}(T)$ is strongly suppressed with increasing $H \parallel [100]$

from 5 to 10.7 T, while changes for $H \parallel [001]$ are much weaker. Figure 4 further verifies that T_1^{-1} for $H \parallel [100]$ is reduced much faster than that for $H \parallel [001]$ with increasing H , and thus the T_1^{-1} anisotropy increases accordingly. As expected, the dashed and dotted lines in Fig. 4 indicate that the T_1^{-1} is almost isotropic for $H=0$. For a quantitative understanding of the anisotropic spin fluctuations, it is convenient to define new spin-lattice relaxation rates: $R_i \equiv T\gamma_n^2 \sum_{\mathbf{q}} A_i^2 \chi''(\mathbf{q}, \omega_0) / \omega_n$, where $i = a, b, c$ represents one of the crystallographic axes, χ'' is the imaginary part of the dynamical susceptibility, and A_i is the hyperfine coupling constant.⁴² This notation emphasizes the fact that T_1^{-1} probes only the SFs perpendicular to the nuclear quantization axis, i.e. $(T_1^{-1})_{[001]} = R_a + R_b$ and $(T_1^{-1})_{[100]} = R_b + R_c$ for a given temperature. Above T_{SO} , our data indicate that $R_a = R_b = R_c$, i.e., isotropic hyperfine coupling and Heisenberg-type SFs. Now, let us take two T_1^{-1} values at 24 K and 10.7 T where T_1^{-1} is different by more than an order of magnitude for the two different field orientations [see Fig. 2(b)]. Then, we have $(R_a + R_b)_{[001]} \approx 10(R_b + R_c)_{[100]}$. With $R_a = R_b$ due to the macroscopic tetragonal symmetry with $H \parallel [001]$, we get $2(R_b)_{[001]} \approx 10(R_b + R_c)_{[100]}$. Therefore, no matter how small R_c may be, $(R_b)_{[001]} \gg (R_b)_{[100]}$. In other words, a field parallel to $[100]$ strongly suppresses all SFs, whereas the spin fluctuations parallel to the CuO_2 planes are not affected for $H \parallel [001]$. This is because the spins are confined to the CuO_2 planes at least below T_{SO} . Due to the strong AFM coupling, the spins orient perpendicular to the external magnetic field. For $H \parallel [001]$, they are already perpendicular, and thus the fluctuations parallel to the planes are not affected by $H \parallel [001]$, and T_1^{-1} is enhanced. In contrast, a field $H \parallel [100]$ creates an in-plane anisotropy that tends to align the spins perpendicular to the field. Now, the spins cannot fluctuate as freely within the planes as for the zero field or as for $H \parallel [001]$, and the larger the applied magnetic field, the stronger is this effect.

Interestingly, we observed a small but clear anomaly at $H_{sf} \approx 7$ T for $H \parallel [100]$, which is attributed to the spin-flop transition.⁹ In the simple stripe picture, the direction of spins alternates between $[100]$ and $[010]$ in neighboring planes owing to the coupling to the LTT structure. For $H \parallel [100]$, spins along $[010]$ are further stabilized, but those along $[100]$ at first are destabilized when the field becomes of the order of the in-plane spin-wave gap. The consequence is a spin-flop transition at $H = H_{sf}$ where these spins change their direction from $[100]$ to $[010]$.⁹ Right at $H_{sf} \approx 7$ T, we indeed observe a local maximum in T_1^{-1} for $H \parallel [100]$, which reflects the enhanced fluctuations of the destabilized spin sublattice. Upon further increasing $H > H_{sf}$, T_1^{-1} decreases rapidly again reflecting the stabilized spin order, and indicating that now these spins are also stabilized in an in-plane direction perpendicular to the field.

Further evidence for a stabilization of the spin order for large fields parallel to $[100]$ is provided by the strong

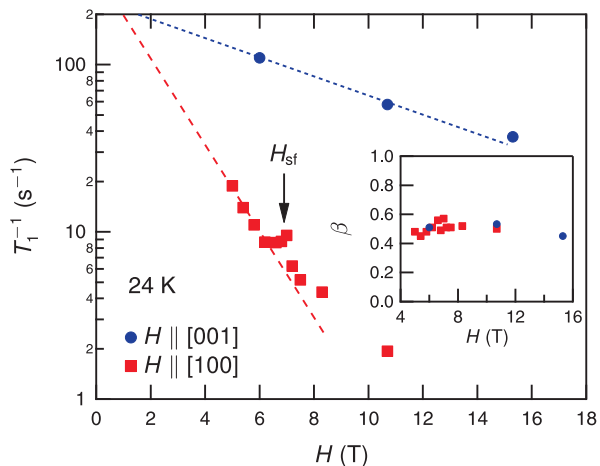


FIG. 4. Detailed field dependence taken at a fixed temperature of 24 K [see the green vertical arrow in Fig. 2(b)] reveals that the T_1^{-1} anisotropy rapidly increases with increasing H . Small anomaly at ~ 7 T is ascribed to the spin flop transition. The dotted and dashed lines are guides to the eye. The inset reveals that β is almost independent of H .

anisotropy of the ^{139}La signal intensity below the spin-ordering temperature T_{SO} . As can be seen in Fig. 1, the integrated NMR signal intensity I_{int} for $H \parallel [100]$ is rapidly reduced below T_{SO} , in stark contrast to that for $H \parallel [001]$ which is constant or even appears to increase at low temperatures. Whereas the NMR intensity can be easily affected by the temperature-dependent gain arising from, e.g., the change of the Q factor of the NMR circuit, the relative intensity at a given temperature should not. Therefore, the clearly different temperature dependence of I_{int} for the two field orientations evidences the strong anisotropy of I_{int} at low temperatures. Since the enhancement of the ^{139}La signal intensity is unlikely in-

trinsic, the strong anisotropy is ascribed to the loss of I_{int} for $H \parallel [100]$. This rapidly disappearing ^{139}La signal intensity looks similar to the wipeout of the ^{63}Cu spectra,^{10,12,13} which is caused by a dramatic shortening of the relaxation times (T_2 and T_1) due to a high spectral density of electronic fluctuations at the Larmor frequency.⁴⁰ While this wipeout effect is not known to depend on the field orientation, the loss of the ^{139}La signal intensity for $H \parallel [100]$ differs from that of the ^{63}Cu spectra and may be caused by static internal hyperfine fields that mainly shift, and, due to a distribution of hyperfine fields, may also spread the ^{139}La intensity over a broad frequency range. On the other hand, the significantly larger T_1^{-1} below T_{SO} for $H \parallel [001]$ [see Fig. 2(b)] indicates the persistence of strong spin fluctuations, which could induce incomplete spin ordering in this field direction. Then this naturally accounts for the strongly anisotropic ^{139}La signal intensity below T_{SO} .

In summary, our NMR results reveal the displacive type of all structural phase transitions in $\text{La}_{1.875}\text{Ba}_{0.125}\text{CuO}_4$ and that the local structure is compatible with the average structure determined by diffraction experiments. The slowing down of AFM spin fluctuations below the LTO \rightarrow LTT transition is triggered by the concomitant onset of charge order. Below the spin ordering temperature, T_{SO} , we observed a strong anisotropy of the spin-lattice relaxation rate at large fields. With increasing field, the spin fluctuations are rapidly suppressed for $H \parallel [100]$, while they are weakly suppressed for $H \parallel [001]$. We conclude that the spin order is stabilized at large fields only for $H \parallel [100]$ involving the spin flop transition at ~ 7 T $\parallel [100]$. Our results resolve the reason for the deviations from the simple BPP model below the spin-ordering temperature.

This work has been supported by the DFG Research Grant No. BA 4927/1-1. M.H. acknowledges support by the Office of Science, U.S. Department of Energy under Contract No. DE-AC02-98CH10886.

* sbaek.fu@gmail.com

- ¹ J. M. Tranquada, B. J. Sternlieb, J. D. Axe, Y. Nakamura, and S. Uchida, *Nature* **375**, 561 (1995).
- ² M. Fujita, H. Goka, K. Yamada, and M. Matsuda, *Phys. Rev. Lett.* **88**, 167008 (2002).
- ³ M. Hückler, G. Gu, J. Tranquada, M. Zimmermann, H.-H. Klauss, N. Curro, M. Braden, and B. Büchner, *Physica C* **460-462**, 170 (2007).
- ⁴ J. Fink, E. Schierle, E. Weschke, J. Geck, D. Hawthorn, V. Soltwisch, H. Wadati, H.-H. Wu, H. A. Dürr, N. Wizen, B. Büchner, and G. A. Sawatzky, *Phys. Rev. B* **79**, 100502 (2009).
- ⁵ T. P. Croft, C. Lester, M. S. Senn, A. Bombardi, and S. M. Hayden, *Phys. Rev. B* **89**, 224513 (2014).
- ⁶ N. B. Christensen, J. Chang, J. Larsen, M. Fujita, M. Oda, M. Ido, N. Momono, E. M. Forgan, A. T. Holmes, J. Mesot, M. Hückler, and M. v. Zimmermann, arXiv: 1404.3192.
- ⁷ V. Thampy, M. P. M. Dean, N. B. Christensen, L. Steinke,

Z. Islam, M. Oda, M. Ido, N. Momono, S. B. Wilkins, and J. P. Hill, *Phys. Rev. B* **90**, 100510 (2014).

- ⁸ M. Hückler, M. v. Zimmermann, Z. J. Xu, J. S. Wen, G. D. Gu, and J. M. Tranquada, *Phys. Rev. B* **87**, 014501 (2013).
- ⁹ M. Hückler, G. D. Gu, and J. M. Tranquada, *Phys. Rev. B* **78**, 214507 (2008).
- ¹⁰ A. W. Hunt, P. M. Singer, K. R. Thurber, and T. Imai, *Phys. Rev. Lett.* **82**, 4300 (1999).
- ¹¹ B. J. Suh, P. C. Hammel, M. Hückler, B. Büchner, U. Ammerahl, and A. Revcolevschi, *Phys. Rev. B* **61**, R9265 (2000).
- ¹² N. J. Curro, P. C. Hammel, B. J. Suh, M. Hückler, B. Büchner, U. Ammerahl, and A. Revcolevschi, *Phys. Rev. Lett.* **85**, 642 (2000).
- ¹³ A. W. Hunt, P. M. Singer, A. F. Cederström, and T. Imai, *Phys. Rev. B* **64**, 134525 (2001).
- ¹⁴ B. Simović, P. C. Hammel, M. Hückler, B. Büchner, and

- A. Revcolevschi, Phys. Rev. B **68**, 012415 (2003).
- ¹⁵ V. F. Mitrović, M.-H. Julien, C. de Vaulx, M. Horvatić, C. Berthier, T. Suzuki, and K. Yamada, Phys. Rev. B **78**, 014504 (2008).
 - ¹⁶ B. Büchner, M. Breuer, A. Freimuth, and A. P. Kampf, Phys. Rev. Lett. **73**, 1841 (1994).
 - ¹⁷ H.-H. Klauss, W. Wagener, M. Hillberg, W. Kopmann, H. Walf, F. J. Litterst, M. Hücker, and B. Büchner, Phys. Rev. Lett. **85**, 4590 (2000).
 - ¹⁸ M. Hücker, M. v. Zimmermann, M. Debessai, J. S. Schilling, J. M. Tranquada, and G. D. Gu, Phys. Rev. Lett. **104**, 057004 (2010).
 - ¹⁹ Z. Guguchia, A. Maisuradze, G. Ghambashidze, R. Khasanov, A. Shengelaya, and H. Keller, New J. Phys. **15**, 093005 (2013).
 - ²⁰ D. Fausti, R. I. Tobey, N. Dean, S. Kaiser, A. Dienst, M. C. Hoffmann, S. Pyon, T. Takayama, H. Takagi, and A. Cavalleri, Science **331**, 189 (2011).
 - ²¹ M. Först, R. I. Tobey, H. Bromberger, S. B. Wilkins, V. Khanna, A. D. Caviglia, Y.-D. Chuang, W. S. Lee, W. F. Schlotter, J. J. Turner, M. P. Minitti, O. Krupin, Z. J. Xu, J. S. Wen, G. D. Gu, S. S. Dhesi, A. Cavalleri, and J. P. Hill, Phys. Rev. Lett. **112**, 157002 (2014).
 - ²² G. B. Teitelbaum, I. M. Abu-Shiekah, O. Bakharev, H. B. Brom, and J. Zaanen, Phys. Rev. B **63**, 020507 (2000).
 - ²³ H.-J. Grafe, N. Curro, B. Young, A. Vyalikh, J. Vavilova, G. Gu, M. Hücker, and B. Büchner, Eur. Phys. J. Special Topics **188**, 89 (2010).
 - ²⁴ S.-H. Baek, A. Erb, B. Büchner, and H.-J. Grafe, Phys. Rev. B **85**, 184508 (2012).
 - ²⁵ S.-H. Baek, P. C. Hammel, M. Hücker, B. Büchner, U. Ammerahl, A. Revcolevschi, and B. J. Suh, Phys. Rev. B **87**, 174505 (2013).
 - ²⁶ G. Gu, M. Hücker, Y.-J. Kim, J. Tranquada, Q. Li, and A. Moodenbaugh, J. Cryst. Growth **287**, 318 (2006).
 - ²⁷ W. G. Clark, M. E. Hanson, F. Lefloch, and P. Ségransan, Rev. Sci. Instrum. **66**, 2453 (1995).
 - ²⁸ A. Narath, Phys. Rev. **162**, 320 (1967).
 - ²⁹ E. S. Bozin, R. Zhong, K. R. Knox, G. Gu, J. P. Hill, J. M. Tranquada, and S. J. L. Billinge, Phys. Rev. B **91**, 054521 (2015).
 - ³⁰ S. Katano, J. Fernandez-Baca, S. Funahashi, N. Mri, Y. Ueda, and K. Koga, Physica C **214**, 64 (1993).
 - ³¹ J. D. Axe and M. K. Crawford, J. Low Temp. Phys. **95**, 271 (1994).
 - ³² C. Friedrich, B. Büchner, M. M. Abd-Elmeguid, and H. Micklitz, Phys. Rev. B **54**, R800 (1996).
 - ³³ M. Braden, M. Meven, W. Reichardt, L. Pintschovius, M. T. Fernandez-Diaz, G. Heger, F. Nakamura, and T. Fujita, Phys. Rev. B **63**, 140510 (2001).
 - ³⁴ S. J. L. Billinge, G. H. Kwei, and H. Takagi, Phys. Rev. Lett. **72**, 2282 (1994).
 - ³⁵ D. Haskel, E. A. Stern, D. G. Hinks, A. W. Mitchell, J. D. Jorgensen, and J. I. Budnick, Phys. Rev. Lett. **76**, 439 (1996).
 - ³⁶ D. Haskel, E. A. Stern, F. Dogan, and A. R. Moodenbaugh, Phys. Rev. B **61**, 7055 (2000).
 - ³⁷ S.-W. Han, E. A. Stern, D. Haskel, and A. R. Moodenbaugh, Phys. Rev. B **66**, 094101 (2002).
 - ³⁸ S. Wakimoto, H. Kimura, M. Fujita, K. Yamada, Y. Noda, G. Shirane, G. Gu, H. Kim, and R. J. Birgeneau, J. Phys. Soc. Jpn. **75**, 074714 (2006).
 - ³⁹ M. Hücker, M. v. Zimmermann, G. D. Gu, Z. J. Xu, J. S. Wen, G. Xu, H. J. Kang, A. Zheludev, and J. M. Tranquada, Phys. Rev. B **83**, 104506 (2011).
 - ⁴⁰ M.-H. Julien, A. Campana, A. Rigamonti, P. Carretta, F. Borsa, P. Kuhns, A. P. Reyes, W. G. Moulton, M. Horvatić, C. Berthier, A. Vietkin, and A. Revcolevschi, Phys. Rev. B **63**, 144508 (2001).
 - ⁴¹ J. M. Tranquada, G. D. Gu, M. Hücker, Q. Jie, H.-J. Kang, R. Klingeler, Q. Li, N. Tristan, J. S. Wen, G. Y. Xu, Z. J. Xu, J. Zhou, and M. v. Zimmermann, Phys. Rev. B **78**, 174529 (2008).
 - ⁴² S.-H. Baek, H. Sakai, E. D. Bauer, J. N. Mitchell, J. A. Kennison, F. Ronning, and J. D. Thompson, Phys. Rev. Lett. **105**, 217002 (2010).